

## Article

# Prospective Prediction of Dapaconazole Clinical Drug–Drug Interactions Using an In Vitro to In Vivo Extrapolation Equation and PBPK Modeling

Natalícia de Jesus Antunes <sup>1,\*</sup>, Fernanda de Lima Moreira <sup>2</sup>, Karin Kipper <sup>3</sup>, Lewis Couchman <sup>4,5</sup>, Daniel Temponi Lebre <sup>6</sup>, Atholl Johnston <sup>4,7</sup> and Gilberto De Nucci <sup>1,8,9</sup>

<sup>1</sup> Department of Pharmacology, Faculty of Medical Sciences, State University of Campinas (UNICAMP), Campinas 13083-881, SP, Brazil

<sup>2</sup> Faculty of Pharmacy, Federal University of Rio de Janeiro, Rio de Janeiro 21941-902, RJ, Brazil

<sup>3</sup> Institute of Chemistry, University of Tartu, 14a Ravila Street, 50411 Tartu, Estonia

<sup>4</sup> Analytical Services International (ASI) Ltd., St George's—University of London, Cranmer Terrace, London SW17 0RE, UK

<sup>5</sup> Pharmaceutical Sciences Clinical Academic Group, King's College London, London SE1 9NH, UK

<sup>6</sup> Center for Applied Mass Spectrometry (CEMSA), São Paulo 05508-000, SP, Brazil

<sup>7</sup> Clinical Pharmacology, William Harvey Research Institute, Barts and The London School of Medicine and Dentistry, Queen Mary University of London, London EC1M 6BQ, UK

<sup>8</sup> Institute of Biomedical Sciences, University of São Paulo (USP), São Paulo 05508-000, SP, Brazil

<sup>9</sup> Faculty of Medicine, São Leopoldo Mandic (SLMANDIC), Campinas 13045-755, SP, Brazil

\* Correspondence: natalicija@gmail.com; Tel.: + 55-19-3251-7373

**Abstract:** This study predicted dapaconazole clinical drug–drug interactions (DDIs) over the main Cytochrome P450 (CYP) isoenzymes using static (in vitro to in vivo extrapolation equation, IVIVE) and dynamic (PBPK model) approaches. The in vitro inhibition of main CYP450 isoenzymes by dapaconazole in a human liver microsome incubation medium was evaluated. A dapaconazole PBPK model (Simcyp version 20) in dogs was developed and qualified using observed data and was scaled up for humans. Static and dynamic models to predict DDIs following current FDA guidelines were applied. The in vitro dapaconazole inhibition was observed for all isoforms investigated, including CYP1A2 (IC<sub>50</sub> of 3.68 μM), CYP2A6 (20.7 μM), 2C8 (104.1 μM), 2C9 (0.22 μM), 2C19 (0.05 μM), 2D6 (0.87 μM), and 3A4 (0.008–0.03 μM). The dynamic (PBPK) and static DDI mechanistic model-based analyses suggest that dapaconazole is a weak inhibitor (AUCR > 1.25 and <2) of CYP1A2 and CYP2C9, a moderate inhibitor (AUCR > 2 and <5) of CYP2C8 and CYP2D6, and a strong inhibitor (AUCR ≥ 5) of CYP2C19 and CYP3A, considering a clinical scenario. The results presented may be a useful guide for future in vivo and clinical dapaconazole studies.

**Keywords:** dapaconazole; cytochrome P450; inhibition; in vitro evaluation; human liver microsomes; IVIVE; PBPK model



**Citation:** Antunes, N.d.J.; Moreira, F.d.L.; Kipper, K.; Couchman, L.; Lebre, D.T.; Johnston, A.; De Nucci, G. Prospective Prediction of Dapaconazole Clinical Drug–Drug Interactions Using an In Vitro to In Vivo Extrapolation Equation and PBPK Modeling. *Pharmaceuticals* **2023**, *16*, 28. <https://doi.org/10.3390/ph16010028>

Academic Editor: Natalia V. De Moraes

Received: 6 November 2022

Revised: 15 December 2022

Accepted: 22 December 2022

Published: 26 December 2022



**Copyright:** © 2022 by the authors. Licensee MDPI, Basel, Switzerland. This article is an open access article distributed under the terms and conditions of the Creative Commons Attribution (CC BY) license (<https://creativecommons.org/licenses/by/4.0/>).

## 1. Introduction

Dapaconazole, a novel imidazole, has shown antifungal activity against several pathogenic fungi, such as *Tricophyton verrucosum*, *Tricophyton rubrum*, *Tricophyton mantagrophutes*, *Microsporum gypseum*, *Microsporum canis*, and *Aspergillus niger* [1–7]. Dapaconazole demonstrated noninferior efficacy to miconazole for the topical treatment of tinea cruris [4], to ketoconazole for treating interdigital tinea pedis [3], and pityriasis versicolor [5]. In addition, dapaconazole has shown a good safety profile in all trials.

Current concern about the use of azole antifungals in clinical practice is the many drug–drug interactions (DDIs) related to these drugs, mainly as moderate/strong inhibitors of cytochrome P450 (CYP) isoenzymes [8,9]. The investigation of a potential DDI of a new azole antifungal in the early drug development process is critical to allow the safe use

of the new molecular entity during clinical trials and later during clinical practice [10]. Therefore, understanding and identifying the enzymes that are inhibited in the presence of the drug under study is directly related to deciding whether to proceed or not in the development phase [11]. Mechanistic approaches such as static (in vitro to in vivo extrapolation equations, IVIVE) or dynamic models (physiologically-based pharmacokinetic (PBPK) models) incorporating in vitro data of human systems are being used increasingly to predict the clinical DDI potential associated with new chemical entities to help in the drug development process [12,13].

This work aimed to predict dapaconazole clinical DDIs over the main CYP450 isoenzymes using static (IVIVE) and dynamic (PBPK model) approaches.

## 2. Results

### 2.1. *In Vitro* DDI

Table 1 summarizes the conditions of the in vitro CYP450 metabolism inhibition assay.

**Table 1.** Conditions of the in vitro CYP450 metabolism inhibition assay.

CYP450 Isoform	Substrate	Substrate Concentration ( $\mu\text{M}$ )	Marker	Inhibitor	Inhibitor Concentration ( $\mu\text{M}$ )	Microsome Concentration (mg/mL)	Incubation Time (min)	Internal Standard (Solvent)
1A2	Phenacetin	12.03	Acetaminofen	Furafylline	0.1–2.3	0.3	30	Sulindac (MTBE)
2A6	Coumarin	2.3	7-Hydroxycoumarin	Tranlycypromine	0.1–2.0	0.3	30	Dextrorphan (EA)
2B6	Bupropion	81.7	Hydroxybupropion	Clopidogrel	0.01–0.05	0.1	10	Sulindac (ACN)
2C8	Paclitaxel	10.0	6 $\alpha$ -Hydroxypaclitaxel	Quercetin	1–5	0.4	20	Dextrorphan (EA)
2C9	Diclofenac	4.04	4'-Hydroxydiclofenac	Sulfaphenazole	0.1–2.0	0.1	10	Sulindac (CF <sup>1</sup> )
2C19	S-mephenytoin	57.2	4'-Hydroxymephenytoin	Tranlycypromine	5–45	0.2	40	Dextrorphan (EA)
2D6	Bufuralol	5.4	1'-Hydroxybufuralol	Quinidine	0.001–0.3	0.25	30	Dextrorphan (EA <sup>2</sup> )
3A	Midazolam	2.27	1-Hydroxymidazolam	Ketoconazole	0.01–0.05	0.1	5	Diazepam (EA)
3A	Nifedipine	7.0	Dehydronifedipine	Ketoconazole	0.01–0.05	0.15	15	Diazepam (EA)

Modifier: <sup>1</sup> HCl 0.5 M; <sup>2</sup> NaOH 1.25  $\mu\text{M}$ . MTBE, methyl tert-butyl ether; EA, ethyl acetate; ACN, acetonitrile; CF, chloroform.

The LC-MS/MS conditions are described in Table 2.

**Table 2.** LC-MS/MS conditions.

CYP Isoform	Marker	MRM Transitions	CE (Volts)	CXP (Volts)
1A2	Acetaminofen	152.11 > 109.90	23	08
		152.11 > 65.20	43	04
2A6	7-Hydroxycoumarin	162.99 > 107.00	31	08
		162.99 > 77.10	47	06
2B6	Hydroxybupropion	256.22 > 238.00	17	14
		256.22 > 238.00	35	12
2C8	6 $\alpha$ -Hydroxypaclitaxel	870.42 > 139.00	21	08
		870.42 > 104.90	77	10
2C9	4'-Hydroxydiclofenac	312.02 > 231.10	27	14
		312.02 > 231.10	43	20
2C19	4'-Hydroxymephenytoin	235.11 > 150.10	25	12
		235.11 > 141.00	15	10
2D6	1'-Hydroxybufuralol	278.25 > 186.00	25	26
		278.25 > 159.00	33	12
3A <sup>1</sup>	1-Hydroxymidazolam	342.06 > 234.00	31	14
		342.06 > 108.90	45	08
3A <sup>2</sup>	Dehydronifedipine	345.00 > 283.90	35	10
		345.00 > 267.80	26	08
IS	Diazepam	285.12 > 154.10	37	10
		285.12 > 193.00	43	16
IS	Sulindac	357.14 > 233.10	59	16
		357.14 > 233.10	47	14
IS	Dextrorphan	258.30 > 157.10	49	10
		258.30 > 199.10	37	18

<sup>1</sup> Midazolam as substrate; <sup>2</sup> Nifedipine as substrate; CE, collision energy; CXP, collision cell exit potential; and IS, internal standard.

The IC<sub>50</sub> values of the dapaconazole inhibition of CYP450 isoforms obtained in vitro are shown in Table 3. Inhibition was observed for all isoforms investigated, CYP1A2 (3.68  $\mu$ M), CYP2A6 (20.7  $\mu$ M), 2C8 (104.1  $\mu$ M), 2C9 (0.22  $\mu$ M), 2C19 (0.05  $\mu$ M), 2D6 (0.87  $\mu$ M), and 3A4 (0.008–0.03  $\mu$ M). The positive inhibitors furafylline (CYP1A2), tranylcyromine (CYP2A6 and CYP2C19), quercetin (CYP2C8), sulfaphenazole (CYP2C9), quinidine (CYP2D6), and ketoconazole (CYP3A) have been shown to be potent inhibitors.

**Table 3.** IC<sub>50</sub> values obtained from the in vitro CYP450 metabolism inhibition assays.

CYP Isoform	IC <sub>50</sub> ( $\mu$ M) Dapaconazole	IC <sub>50</sub> ( $\mu$ M) Positive Control
1A2	3.682 (0.1295)	0.5847 (0.08698)—Furafylline
2A6	20.7 (0.0561)	0.7994 (0.08698)—Tranylcyromine
2C8	104.1 (0.4935)	0.6221 (0.5273)—Quercetin
2C9	0.2186 (0.1047)	0.4467 (0.3811)—Sulfaphenazole
2C19	0.05297 (0.01904)	0.4467 (0.3811)—Tranylcyromine
2D6	0.8675 (0.2102)	0.03712 (0.07987)—Quinidine
3A <sup>1</sup>	0.007693 (0.001267)	0.003445 (1.161)—Ketoconazole
3A <sup>2</sup>	0.03032 (0.05029)	0.003667 (0.3481)—Ketoconazole

<sup>1</sup> Midazolam as substrate; and <sup>2</sup> Nifedipine as substrate.

## 2.2. Development of PBPK Model in Dogs

A PBPK model was first developed in dogs using a hybrid PBPK approach employing the in vivo clearance reported in dogs [7]. The input parameters are described in Table 4.

**Table 4.** Input parameters for the dapaconazole PBPK model in dogs and humans.

Parameters	Dog Model		Human Model	
	Value	Reference	Value	Reference
<b>Physical chemistry</b>				
Molecular weight (g/mol)	415.2	Drugbank	415.2	Drugbank
log P	5.63	Drugbank	5.63	Drugbank
pKa (monoprotic base)	6.77	Drugbank	6.77	Drugbank
Unbound fraction	0.037	Antunes et al. [14]	0.077	Antunes et al. [14]
Blood/Plasma	1 *	Assumed	6.08	Simcyp predicted
<b>Distribution</b>				
	Minimal + SAC model		Minimal+ SAC model	
$V_{ss}$ (L/kg)	6.359	Predicted Method 2	6.35	Simcyp Allometry (simple allometry)
$V_{sac}$ (L/kg)	3.883	Best fit	3.883	Allometry
$K_{in}/K_{out}$ (1/h)	0.0262/0.01582	Best fit	0.0262/0.01582	Allometry
$K_p$	0.01	Best fit	0.01	Allometry
<b>Elimination</b>				
CL IV (L/h)	According to IV dose simulated	Palo et al. [7]	35.5	Simcyp Allometry (simple allometry)
CL int. mic. $\mu$ L/min/mg	258	Antunes et al. [14]	118.5	Antunes et al. [14]
$f_{u,inc}$	0.97	Antunes et al. [14]	0.94	Antunes et al. [14]

\* This value was assumed 1 as a default value provided by Simcyp due to the lack of experimental data.  $V_{ss}$ , volume of distribution at steady-state conditions; SAC, single adjusting compartment;  $V_{sac}$ , apparent volume of SAC;  $K_{in}/K_{out}$ , rate constant from systemic compartment to SAC/rate constant from SAC compartment to the systemic compartment;  $K_p$ , tissue-to-plasma partition coefficient; CL IV, intravenous clearance; CL int. mic., intrinsic clearance obtained from liver microsomes; and  $f_{u,inc}$ , unbound fraction.

First, we used the raw data from Palo et al. [7] to obtain the dapaconazole compartmental model employing Phoenix<sup>®</sup> WinNonlin<sup>®</sup>, version 6.3 (Certara). The intravenous dapaconazole exposure was described as a bicompartmental model (data not shown). The PBPK model was first developed using a single 2 mg/kg intravenous dose of dapaconazole and employing the reported in vivo clearance of 591.7 L/min [7] in a hybrid approach. Then, the full PBPK model, which used the method 2 (Rodgers and Rowland [15]) to predict the volume of distribution at steady-state conditions ( $V_{ss}$ ) was evaluated. The sensitivity analysis estimated the tissue-to-plasma partition coefficient ( $K_p$ ) value of 0.01 to best fit the observed values. Despite that, the full PBPK model did not describe the dapaconazole bicompartmental profile. Considering this issue, in addition to the low volume of distribution ( $V_d$ ) observed in dogs, the minimal PBPK plus a single adjusting compartment (SAC) was selected. The  $V_{sac}$  (apparent volume of SAC),  $k_{in}$  (rate constant from systemic compartment to SAC), and  $k_{out}$  (rate constant from SAC compartment to the systemic compartment) values were determined from the parameter estimation approach selecting the values of 3.88 L/kg,  $0.026\text{ h}^{-1}$ , and  $0.016\text{ h}^{-1}$ , respectively, that better described the observed PK profile. The predicted  $V_{ss}$  using Rodgers and Rowland's method [15] was 6.36 L/kg. The developed PBPK model described the observed dapaconazole PK profile in dogs reasonably well after intravenous single doses of 1 mg/kg, 2 mg/kg, or 20 mg/kg (Figure 1); furthermore, the PK parameters' observed/predicted ratios were between 0.5-fold to 2-fold (Table 5).

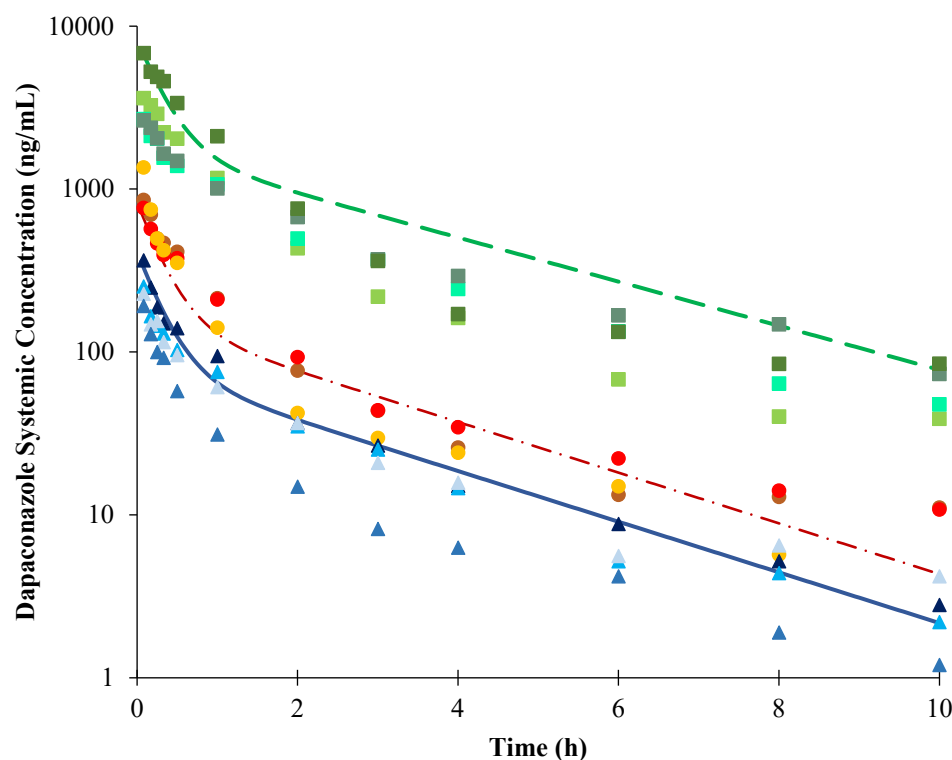


**Figure 1.** Plasma concentrations versus time plots for dapaconazole after intravenous dose administration in dogs. The markers represent the observed data in dogs from Palo et al. [7], and the lines represent the predicted mean concentration versus time profiles obtained with the PBPK model. The solid line and triangle markers represent predicted and observed plasma concentrations after a 1 mg/kg dose; the dash-dot line and circle markers represent predicted and observed plasma concentrations after a 2 mg/kg dose; and the dashed line and square markers represent predicted and observed plasma concentrations after a 20-mg/kg dose.

**Table 5.** Prediction performance of the dapaconazole PBPK model in dogs (model qualification).

Intravenous Dose	1 mg/kg			
Parameters	AUC <sub>0-t</sub> (ng/mL.h)	C <sub>max</sub> (ng/mL)	CL (mL/min)	t <sub>1/2</sub> Terminal (h)
Predicted	306.7	404.7	543.5	1.9
Observed <sup>1</sup>	255.0	373.2	700.0	2.1
Observed/predicted ratio	0.83	0.92	1.29	1.08
	2 mg/kg			
Predicted	613.3	809.3	543.5	1.9
Observed <sup>1</sup>	779.9	1444.7	591.7	2.5
Observed/predicted ratio	1.27	1.78	1.09	1.29
	20 mg/kg			
Predicted	7331.2	8097.3	454.7	2.2
Observed <sup>1</sup>	4780.1	4708.3	700.0	2.3
Observed/predicted ratio	0.65	0.58	1.54	1.04

<sup>1</sup> Data from Palo et al. [7]. AUC<sub>0-t</sub>, the area under the curve zero to last time of sample collected; C<sub>max</sub>, maximum plasma concentration; and CL, clearance; and t<sub>1/2</sub> terminal, terminal half-life.

To predict the role of CYP450 liver enzymes on the elimination of dapaconazole in dogs, the intrinsic clearance value obtained from dog liver microsomes (257.97  $\mu$ L/min/mg) [14] was incorporated as the single elimination pathway in dogs. The predicted systemic clearance obtained after a single intravenous dose of 20 mg/kg dapaconazole from the model incorporating intrinsic clearance from dog liver microsomes in an in vitro model

(164 mL/min) was 3.3-fold lower than the predicted systemic clearance (454.7 mL/min) from the model incorporating in vivo clearance in dogs. Considering this, the in vivo clearance value in dogs, and not intrinsic clearance from the microsome, was applied in the allometric scaling formula to predict clearance in humans.

### 2.3. Extrapolation of the PBPK Model Developed in Dogs to Humans

The allometry tools provided by Simcyp were employed to extrapolate the  $V_{ss}$  and clearance (CL) from dogs to humans. Simple allometry with one species (dog) considered  $V_{ss, human} = V_{ss, animal} (L/kg)$  [16], and  $CL_{human} = CL_{animal} (mL/day)$  [17]. The input parameters included in the dapaconazole PBPK model for humans are described in Table 4.

To predict the role of CYP450 liver enzymes in the elimination of dapaconazole in humans, the intrinsic clearance value obtained from human liver microsomes (118.5  $\mu L/min/mg$ ) [14] was incorporated as the single elimination pathway in humans.

The elimination half-life ( $t_{1/2}$ ) observed after simulating a single 20 mg/kg intravenous dose of (in an adult of 73 kg corresponding to a 1.460-mg dose) dapaconazole was 7.9 h. As an exercise in the simulation of potential DDI, we selected an intravenous dose of 500 mg every 8 h as a dosing regimen.

### 2.4. DDI Prediction of Dapaconazole as an Inhibitor

First, dapaconazole inhibition potential was evaluated by calculating the R1 value for reversible inhibition, demonstrating that dapaconazole has clinical inhibition potential in all CYP isoforms tested, except CYP2C8. To assess the clinical potential interaction of dapaconazole to the exposure (area under the curve ratio—AUC) of CYP substrate drugs, dapaconazole was evaluated as an inhibitor using static and dynamic models to predict DDI in clinical scenarios (Table 6) [18]. Considering both results from static and dynamic models, the worst-case scenario (higher AUCR value) was considered to classify the potential of dapaconazole as an inhibitor according to FDA classification [13]. Dapaconazole is a potential clinically weak inhibitor of CYP1A2 and CYP2C9, a moderate inhibitor of CYP2D6 and CYP2C8, and a strong inhibitor of CYP2C19 and CYP3A4.

**Table 6.** Evaluation of the potential of dapaconazole as a CYP inhibitor through the predicted area under the curve ratios using a static and dynamic model.

CYP	Substrate	[I]( $\mu M$ )	Ki ( $\mu M$ )	R1	fm	Static AUCR	Dynamic AUCR	FDA Classification [13]
1A2	Phenacetin	9.5	1.84	1.20	0.71	1.86	1.17	Weak
2C8	Paclitaxel	9.5	52.05	1.01	0.5	3.00	1.46 <sup>1</sup>	Moderate
2C9	Diclofenac	9.5	0.11	4.43	0.87	1.95	1.38 <sup>2</sup>	Weak
2C19	S-Mephenytoin	9.5	0.03	15.14	0.89	3.86	5.36	Strong
2D6	Bufuralol	9.5	0.43	1.86	0.66	2.31	1.51	Moderate
3A4	Midazolam	9.5	0.004	98.26	0.88	19.45	5.14	Strong
3A4	Nifedipine	9.5	0.02	25.70	0.96	5.31	4.05	Strong

<sup>1</sup> AUCR dynamic study was performed in Simcyp using repaglinide as a CYP2C8 substrate. <sup>2</sup> AUCR dynamic study was performed in Simcyp using tolbutamide as a CYP2C9 substrate. Abbreviations: R1, ratio of intrinsic clearance values of a probe substrate for an enzymatic pathway in the absence and the presence of dapaconazole; CYP, cytochrome P450; fm, fraction metabolized; [I], inhibitor concentration that is the total plasma maximum concentration ( $C_{max}$ ); Ki, inhibition constant; and AUCR, area under the curve ratio between AUC with inhibitor and AUC without inhibitor. Notes: Ki was corrected to the unbound value using the in vitro unbound fraction ( $f_{u,inc}$ ) of 0.94  $Ki = IC_{50}/2$ ; the mean  $C_{max}$  of 9.5  $\mu M$  in humans was obtained from simulations of 500 mg every 8 h and corrected by multiplying the ratio of unbound fraction in plasma ( $f_u$ ) with the blood-to-plasma ratio (Rb); the fm of nifedipine, midazolam, phenacetin, S-mephenytoin, and bufuralol were adapted from Simcyp. Paclitaxel was extracted from Hua et al. [19]; and diclofenac from Siu and Lai [20]. AUCR > 1.25 and <2: weak inhibitor; AUCR > 2 and <5: moderate inhibitor; and AUCR  $\geq$  5: strong inhibitor.

## 3. Discussion

Azole antifungals are used as a primary treatment for fungal infections, and to support the treatment of immune-suppressed patients, for example, organ transplant patients and patients with acquired immunodeficiency syndrome, who also use other medications. Azole antifungals can change the exposure of these medications due to DDIs caused by

inhibiting drug-metabolizing enzymes [9,21]. Drug interactions represent a major problem in drug therapy. Therefore, prior knowledge of these interactions during the development process of new drugs through in vitro enzyme inhibition studies is of great value, as this helps in avoiding adverse reactions generated by the interactions [22].

Dapaconazole is metabolized by CYP450 enzymes in the liver as previously demonstrated by our research group using in vitro studies with liver microsomes from humans, dogs, and rats [14]. Other azole antifungals such as itraconazole and voriconazole also are substrates of CYP450 enzymes. In addition, azole antifungals are well-known CYP450 inhibitors, and the inhibition of CYP3A4 enzymatic activity is considered the main source of DDIs by these drugs [23–27].

In liver microsomes, the inhibitory potency of a drug can be measured by determining the inhibition constant required to achieve half the maximum inactivation rate for reversible inhibition ( $K_i$ ) or  $IC_{50}$  of a specific substrate for each CYP isoform.  $IC_{50}$  values are typically classified into low ( $IC_{50} > 10 \mu\text{M}$ ), moderate ( $1 \mu\text{M} < IC_{50} < 10 \mu\text{M}$ ), and high ( $IC_{50} < 1 \mu\text{M}$ ) reversible inhibition [11]. Considering these values, dapaconazole in vitro slightly inhibits CYP2A6 and CYP2C8, moderately inhibits CYP1A2, and highly inhibits CYP2C9, CYP2C19, CYP2D6, and CYP3A. Comparing dapaconazole with other azole antifungals evaluated in vitro, fluconazole moderately inhibits CYP2C9 and CYP3A; itraconazole strongly inhibits CYP2B6 and CYP3A; ketoconazole strongly inhibits CYP1A1 and CYP3A and moderately inhibits CYP1A2, CYP2A6, and CYP2C9; miconazole strongly inhibits CYP2A6, CYP2B6, CYP2C9, CYP2C19, CYP2D6, and CYP3A; posaconazole strongly inhibits CYP3A; and voriconazole strongly inhibits CYP2B6 and CYP3A, and moderately inhibits CYP2C9 and CYP2C19 [9].

Considering that one important application of the PBPK model during early drug development is to predict drug exposure prior to in vivo studies (mainly clinical trials), we employed this valuable tool to build a dapaconazole PBPK model in dogs, and recently it was extrapolated to humans in order to predict potential DDI scenarios in humans. The PBPK model developed in dogs, using a middle-out approach considering the observed in vivo clearance previously reported by Palo et al. [7], was qualified with the observed data through a visual predictive check and 0.5- to 2-fold ratio difference observed to predict the pharmacokinetic parameter value (Figure 1 and Table 5).

After developing and qualifying the PBPK model in dogs, we extrapolated the model to humans, assuming the same CL and  $V_{ss}$  values from dogs. Other input parameters for the dapaconazole PBPK model in humans are described in Table 4. Later, we extrapolated this PBPK model to humans to perform a prospective clinical DDI prediction obtaining the AUCR dynamic (Table 6).

The DDI potential analysis from  $K_i$  and R1 values (Table 6) indicates that dapaconazole has a low potential to inhibit CYP2C8 ( $K_i$ : 52.1  $\mu\text{M}$ ; R1: 1.01), while it has a moderate potential to inhibit CYP1A2 ( $K_i$ : 1.84  $\mu\text{M}$ ; R1: 1.20) and high potential to inhibit CYP2C9 ( $K_i$ : 0.11  $\mu\text{M}$ ; R1: 4.43), CYP2C19 ( $K_i$ : 0.03  $\mu\text{M}$ ; R1: 15.14), CYP2D6 ( $K_i$ : 0.43  $\mu\text{M}$ ; R1: 1.86), and CYP3A ( $K_i$ : 0.004  $\mu\text{M}$ ; R1: 98.26 for midazolam substrate;  $K_i$ : 0.015  $\mu\text{M}$ ; R1: 25.70 for nifedipine substrate).

The results of the DDI static and dynamic mechanistic models indicated that dapaconazole is a weak inhibitor of CYP1A2 and CYP2C9, a moderate inhibitor of CYP2C8 and CYP2D6, and a strong inhibitor of CYP2C19 and CYP3A, according to FDA guidelines [13]. In general, the AUCR static and dynamic values for each CYP isoform evaluated correlated reasonably well. To critically evaluate these results, it is important to highlight that the static model considers the worst-case scenario, assuming that the inhibitor concentration is maintained at the maximum plasma concentration ( $C_{max}$ ) throughout the entire timed course, while the dynamic model uses the concentration versus time profiles of both inhibitor and substrate drugs, giving a more realistic prediction of a clinical DDI. Considering the  $AUCR \geq 1.25$  values obtained, we indicate that a clinical DDI study using a sensitive index substrate should be further performed for all CYP isoforms evaluated in the current work.

Clinical DDI studies demonstrated that fluconazole, itraconazole, ketoconazole, posaconazole, and voriconazole are moderate to strong CYP3A inhibitors, and fluconazole, itraconazole, ketoconazole, miconazole, and voriconazole are moderate CYP2C9 inhibitors [9]. The findings of the present study indicate that dapaconazole has the same characteristics as other azoles as an inhibitor of many CYP isoforms with a moderate to strong inhibition in CYP3A, but a weak inhibition in CYP2C9.

## 4. Materials and Methods

### 4.1. Chemicals and Reagents

Dapaconazole was obtained from Biolab Sanus Farmacêutica Ltd.a. (São Paulo, Brazil). Acetaminophen, bufuralol, coumarin, dextrorphan, diazepam, 4'-hydroxydiclofenac, ketoconazole, midazolam, 1-hydroxymidazolam, paclitaxel, phenacetin, sulindac, and formic acid (99% to 100%) were obtained from Sigma-Aldrich (St Louis, MO, USA). Nifedipine and dehydronifedipine were purchased from Cayman Chemical (Ann Arbor, MI, USA). Bupropion, clopidogrel, quinidine, sulfaphenazole, 4'-hydroxymephenytoin, 7-hydroxycoumarin, hydroxybupropion, 6 $\alpha$ -hydroxypaclitaxel, and 1'-hydroxybufuralol, were purchased from Toronto Research Chemicals (Toronto, ON, Canada). Diclofenac, furafylline, S-mephenytoin, quercetin, and tranlycypromine were purchased from Santa Cruz Biotechnology (Dallas, TX, USA). The HPLC-grade solvents acetonitrile, ethyl acetate, methyl tert-butyl ether, chloroform, and methanol were obtained from Rathburn Chemicals (Walkerburn, Scotland). Aqueous phosphate buffer (0.5 mol/L, pH 7.4), reduced nicotinamide adenine dinucleotide phosphate (NADPH) regenerating system solutions A and B, and pooled HLMs (150 donors pool), RLMs (male pool), and BLMs (male pool) were purchased from Corning (Woburn, MA, USA). Deionized water was obtained in-house using a Synergy UV<sup>®</sup> purification system (Millipore, Molsheim, France).

The standard stock solutions of the probe substrates were prepared in methanol at the following concentrations: phenacetin 5 mg/mL, coumarin 2 mg/mL, bupropion 5 mg/mL, paclitaxel 1 mg/mL, diclofenac 2 mg/mL, S-mephenytoin 5 mg/mL, bufuralol 1 mg/mL, midazolam 100  $\mu$ g/mL, and nifedipine 1 mg/mL. The standard stock solutions of the markers (acetaminophen, 7-hydroxycoumarin, hydroxybupropion, 6 $\alpha$ -hydroxypaclitaxel, 4'-hydroxydiclofenac, 4'-hydroxymephenytoin, 1'-hydroxybufuralol, 1'-hydroxymidazolam, and dehydronifedipine) were prepared in methanol at 1mg/mL. The standard stock solutions of the inhibitors were prepared in methanol at the following concentrations: furafylline 5 mg/mL, tranlycypromine 1 mg/mL, clopidogrel 1 mg/mL, quercetin 5 mg/mL, sulfaphenazole 1 mg/mL, quinidine 2 mg/mL, and ketoconazole (1 mg/mL). The standard stock solutions of the internal standards (IS) were prepared in methanol at the following concentrations: sulindac 1 mg/mL, dextrorphan 5 mg/mL, and diazepam 1 mg/mL. All solutions were stored in amber vials at  $-20^{\circ}\text{C}$ .

### 4.2. In Vitro DDI

To identify the potential of dapaconazole to inhibit CYP450, the activity of CYP1A2, CYP1A6, CYP2C8, CYP2C9, CYP2C19, CYP2D6, and CYP3A4/5 was evaluated in HLM using selective substrates in concentrations near to their  $K_m$  and inhibitors (positive control) of CYP450, as shown in Table 1. The incubation conditions employed for each CYP450 isoform were performed, as previously described [28–35].

Solutions ( $n = 3$ ) containing 10  $\mu$ L of probe substrate of each CYP450 isoform with or without 10  $\mu$ L dapaconazole (0.01, 0.1, 1, 10, and 100  $\mu$ M) or specific inhibitors were added to 1.5 mL propylene tubes and evaporated to dryness. Buffer solution (0.1 mol/L aqueous phosphate buffer, pH 7.4, 69  $\mu$ L), NADPH-regenerating solutions (10  $\mu$ L solution A: 26 mmol/L NADP<sup>+</sup>, 66 mmol/L glucose-6-phosphate, and 66 mmol/L MgCl<sub>2</sub>; 2  $\mu$ L solution B: 40 U/mL glucose-6-phosphate dehydrogenase in 5 mmol/L sodium citrate), and deionized water (69  $\mu$ L) were added, in a total volume of 150  $\mu$ L. The tubes were vortex-mixed and preincubated with continuous gentle shaking for 5 min at 37  $^{\circ}\text{C}$  in a shaking water bath. Reactions were initiated by the addition of 50  $\mu$ L of HLM solution

in the tubes which were gently mixed by hand and incubated with continuous gentle shaking at 37 °C. Aliquots of 200 µL ice-cold solvent (Table 1) containing IS (1 µg/mL) were added. The samples were vortexed for 5 min at 2000 rpm in a VXR basic Vibrax® (Staufen, Germany) and then centrifuged at 16,000 × g (Hettich® MIKRO 185, Tuttlingen, Germany) for 15 min at 25 °C. The supernatants were transferred to glass autosampler vials and submitted to LC-MS/MS analysis (5 µL injection volume) to monitor the substrate metabolite formation.

#### 4.3. Analysis by LC-MS/MS

The liquid chromatography (HPLC) system (Agilent Technologies, Santa Clara, CA, USA) consisted of a 1290 binary LC pump, a 1290 Infinity II Series™ autosampler, and an MCT 1290 column oven. Dapaconazole was separated in a Luna™ Omega polar C18 column (150 × 2.1 mm, 5-µm particle size; Phenomenex, Torrance, CA, USA) held at 40 °C using deionized water + 0.1% formic acid as mobile phase A and acetonitrile + 0.1% formic acid as mobile phase B at a flow rate of 0.3 mL/min. The applied gradient program consisted of 10% B, followed by a linear change to 100% B over 3 min. Mobile phase percentage B was then kept at 100% for 1 min and returned to initial conditions over 0.2 min (total run time of 5 min). The temperature of the autosampler was maintained at 5 °C.

Analytes and ISs were monitored in an API 4000™ triple quadrupole mass-spectrometer (AB Sciex, Concord, ON, Canada) with positive heated ion spray (Positive TurboIonSpray, MH<sup>+</sup>) for analyte detection. Source conditions were gas (high-purity nitrogen) temperature of 300 °C, collision gas of 3 mTorr, and IonSpray voltage of 5000 V. The analysis was performed in multiple reaction monitoring (MRM) mode. The MRM transitions, collision energy (CE), and collision cell exit potential (CXP) are presented in Table 2. The data acquisition and quantification were performed using Analyst™ version 1.3.2 (AB Sciex, Concord, ON, Canada).

#### 4.4. IC<sub>50</sub> Determination

The remaining CYP450 activity was calculated by comparing samples in the presence and absence of dapaconazole or selective inhibitors, according to Equation (1):

$$\%REA = \frac{A_i}{A_0} \cdot 100 \quad (1)$$

where %REA is the percentage of remaining enzymatic activity,  $A_i$  corresponds to the metabolite-to-IS peak area ratio in the presence of dapaconazole or selective inhibitors, and  $A_0$  corresponds to the metabolite-to-IS peak area ratio in the absence of dapaconazole or selective inhibitors.

IC<sub>50</sub> values were determined by a nonlinear regression of the %REA of each CYP450 isoform versus the logarithm of inhibitor concentration, using GraphPad Prism version 5.01 software (GraphPad Software, San Diego, CA, USA).

#### 4.5. PBPK Model Strategy

All modeling was conducted using Simcyp modeling software (v. 20, Certara, Princeton, NJ, US). A PBPK model was constructed to describe the pharmacokinetic profiles of intravenous dapaconazole in dogs, and it was extrapolated to predict drug–drug interactions in humans using a bottom-up approach (Figure 2). All of the input parameters are described in Table 4.

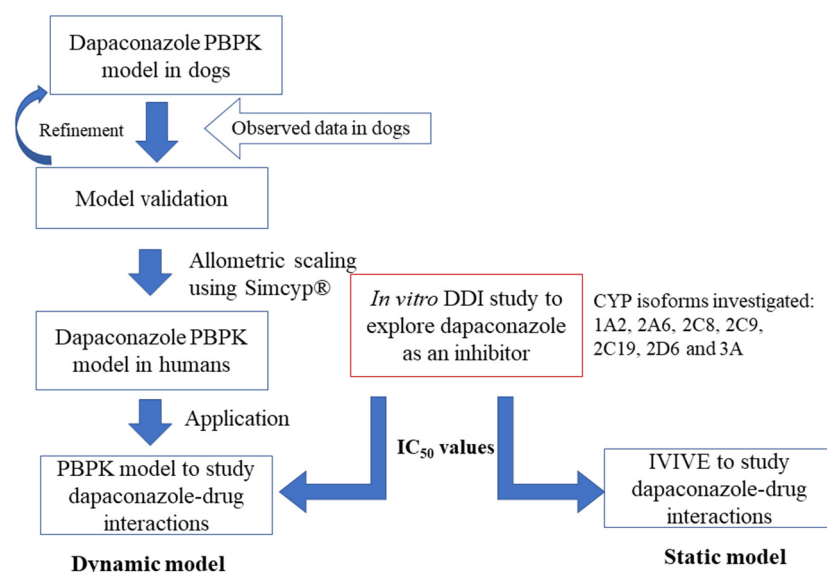


Figure 2. Study workflow.

First, a dog PBPK model was developed to describe the observed dapaconazole PK profile from a published study from our research group [7]. The Simcyp minimal PBPK, which considers all organs other than the intestine and liver as a single compartment [36], plus a SAC distribution model were selected. This model better described the bicompartamental distribution profile of dapaconazole [7]. The  $V_{ss}$  was predicted using Rodgers and Rowland's equations (method 2) [15]. A  $K_p$  scalar was determined to best describe the observed dog data using a sensitivity analysis approach. The final values of  $V_{sac}$ ,  $k_{in}$ , and  $k_{out}$  were determined from the parameter estimation approach selecting the best values to describe the shape of the observed PK profile. For the elimination model development, the *in vivo* systemic clearance values reported in dogs [7] were employed in a middle-out approach. The intrinsic clearance value from dog liver microsomes obtained from a previous study by our research group [14] was employed to test the role of CYP-mediated hepatic clearance in the systemic elimination of dapaconazole in dogs. The PBPK model was evaluated through a visual comparison of observed *in vivo* plasma concentration–time profiles with the concentrations predicted in dogs, and the PK parameters within observed/predicted ratios between 0.5-fold to 2-fold were considered acceptable.

The PBPK model developed in dogs considering the *in vivo* systemic clearance values reported in dogs [7] (middle-out approach) was extrapolated to predict the plasma concentration–time profile in humans and it was used in a prospective prediction of DDI.

The single species allometric scaling tool provided by Simcyp was used to extrapolate the CL and  $V_{ss}$  in dogs to humans based on Equation (2):

$$CL_{hum} = b \times CL_{dog} \left( \frac{BW_{hum}}{BW_{dog}} \right)^a \quad (2)$$

$CL_{hum}$  is the intravenous clearance in humans,  $CL_{dog}$  is the intravenous dog clearance,  $BW_{hum}$  is the human body weight,  $BW_{dog}$  is a dog body weight of 10 kg, and  $a$  and  $b$  are the allometric coefficient and exponent for dapaconazole, respectively.

$$V_{ss,hum} = a \times V_{ss,dog} \quad (3)$$

In Equation (3),  $V_{ss,hum}$  is the steady-state volume of distribution in humans, and  $V_{ss,dog}$  is the steady-state volume of distribution in the dog.

$V_{sac}$ ,  $K_{in}$ , and  $K_{out}$  values were kept as estimated for the dog model. The intrinsic clearance from HLM was also tested as the main elimination route. The Simcyp healthy

volunteer population was considered, selecting individuals aged from 20 to 50 years old and a gender ratio of 1:1 for all the simulations in humans. The mean demographic parameters were 29.5 years old, 73 kg body weight, and 168.3 cm height. Simulations of 10 trials with 10 subjects were conducted with the dosing regimen of intravenous 20 mg/kg single dose or intravenous 500 mg every 8 h.

#### 4.6. Dynamic Model Analysis Using PBPK for DDI Prediction

The potential of dapaconazole to inhibit CYP isoenzymes was predicted using the PBPK model extrapolated to humans. The  $K_i$  input values were estimated from the ratio  $IC_{50}/2$ . Since the  $IC_{50}$  experiments were designed considering the substrate concentration equal to  $K_m$ , the simplification of  $K_i$  as  $IC_{50}/2$  was considered for a competitive inhibition reaction [37]. For the dynamic DDI model, the trial design included multiple intravenous dapaconazole 500 mg administrations every 8 h for 60 h and starting the protocol at 9 AM on day 1. Each CYP substrate (default substrate model provided by Simcyp) was administered at 9 AM on day 3 in a single oral dose in a fasted state: 150 mg phenacetin (CYP1A2), 0.25 mg repaglinide (CYP2C8), 500 mg tolbutamide (CYP2C9), 200 mg S-mephenytoin (CYP2C19), 20 mg bufuralol (CYP2D6), 5 mg midazolam, and 5 mg nifedipine (CYP3A).

The following Equation (4) was considered for the potential DDI evaluation:

$$AUCR = \frac{AUC_{\text{with inhibitor}}}{AUC_{\text{without inhibitor}}} \quad (4)$$

where AUCR is the area under the curve ratio,  $AUC_{\text{with inhibitor}}$  is AUC in the presence of the inhibitor, and  $AUC_{\text{without inhibitor}}$  is AUC in the absence of the inhibitor.

#### 4.7. Static Model Analysis Using IVIVE for DDI Prediction

Initially, the ratio ( $R_1$ ) of intrinsic clearance values of a probe substrate for an enzymatic pathway in the absence and presence of the interacting drug (dapaconazole) for reversible inhibition was calculated according to Equation (5) [13]:

$$R_1 = 1 + (I_{\text{max,u}}/K_{i,u}) \quad (5)$$

where  $I_{\text{max,u}}$  is the maximal unbound plasma concentration of the interacting drug at steady-state conditions, and  $K_{i,u}$  is the unbound inhibition constant determined in vitro.

The static DDI model employed Equation (6) to predict the AUCR:

$$AUCR = 1 / \left( \frac{f_m}{\left(1 + \frac{[I]}{K_i}\right)} + (1 - f_m) \right) \quad (6)$$

where  $[I]$  is the simulated  $C_{\text{max}}$ ,  $K_i$  is the inhibition constant, and  $f_m$  is the fraction metabolized.  $K_i$  was corrected to the unbound value using the in vitro unbound fraction ( $f_{u,\text{inc}}$ ) of 0.94;  $K_i = IC_{50}/2$ . The mean dapaconazole  $C_{\text{max}}$  of 9.5  $\mu\text{M}$  in humans was obtained from simulations of 500 mg every 8 h and corrected by multiplying the ratio of unbound fraction in plasma ( $f_u$ ) (0.037) [14] with the blood-to-plasma ratio ( $R_b$ ) (6.08 predicted with Simcyp). Nifedipine, midazolam, phenacetin, S-mephenytoin, and bufuralol  $f_m$  values were adapted from Simcyp; the paclitaxel  $f_m$  value was extracted from Hua et al. [19]; and the diclofenac  $f_m$  value was extracted from Siu and Lai [20].

#### 4.8. Dapaconazole DDI Results Interpretation

Two recent guidelines provided by the FDA regarding in vitro [13] and clinical [38] DDI studies were considered for interpreting DDI results.

If  $R_1 \geq 1.02$ , the potential DDI should be investigated further either using mechanistic (static and/or dynamic) models.

The AUCRs obtained with static and dynamic models were evaluated according to the following criteria:  $AUCR > 1.25$  and  $< 2$ : weak inhibitor;  $AUCR > 2$  and  $< 5$ : moderate inhibitor; and  $AUCR \geq 5$ : strong inhibitor.

$AUCR \geq 1.25$  based on static or dynamic mechanistic models indicates that a clinical DDI study using a sensitive index substrate should be further performed.

## 5. Conclusions

The isoforms CYP2C19, CYP2D6, and CYP3A4 were highly inhibited by dapaconazole, while CYP1A2 was moderately inhibited, CYP2C9 was weakly inhibited, and CYP1A6 was not inhibited when evaluated under in vitro inhibition studies with human liver microsomes. The hybrid intravenous dapaconazole PBPK model developed in dogs described the observed data reasonably well, and it was scaled up to humans. The dynamic (PBPK) and static DDI mechanistic model-based analysis suggest that dapaconazole is a weak inhibitor of CYP1A2 and CYP2C9, a moderate inhibitor of CYP2C8 and CYP2D6, and a strong inhibitor of CYP2C19 and CYP3A, considering a clinical scenario. The results presented may be a useful guide for future in vivo and clinical dapaconazole studies.

**Author Contributions:** Conceptualization, G.D.N. and N.d.J.A.; methodology, N.d.J.A., F.d.L.M., and D.T.L.; validation, K.K. and L.C.; formal analysis, N.d.J.A. and F.d.L.M.; investigation, N.d.J.A.; resources, A.J. and G.D.N.; data curation, N.d.J.A.; writing—original draft preparation, N.d.J.A. and F.d.L.M.; writing—review and editing, G.D.N., A.J. and N.d.J.A.; visualization, N.d.J.A., K.K. and L.C.; supervision, G.D.N.; project administration, N.d.J.A.; funding acquisition, N.d.J.A. All authors have read and agreed to the published version of the manuscript.

**Funding:** This research was funded by the São Paulo Research Foundation (FAPESP), grant number 2016/22506-1.

**Institutional Review Board Statement:** Not applicable.

**Informed Consent Statement:** Not applicable.

**Data Availability Statement:** Data is contained within the article.

**Acknowledgments:** Jim Hesson copyedited the manuscript (<https://www.academicenglishsolutions.com/editing-service>, accessed on 6 November 2022).

**Conflicts of Interest:** The authors declare no conflict of interest.

## References

1. de Moraes, F.C.; Bittencourt, S.F.; Perissutti, E.; Frecentese, F.; Arruda, A.M.M.; Chen, L.S.; Babadópulos, T.; De Nucci, G. Quantification of Dapaconazole in Human Plasma Using High-Performance Liquid Chromatography Coupled to Tandem Mass Spectrometry: Application to a Phase I Study. *J. Chromatogr. B Anal. Technol. Biomed. Life Sci.* **2014**, *958*, 102–107. [[CrossRef](#)] [[PubMed](#)]
2. Gagliano-Jucá, T.; Arruda, A.M.M.; Sampaio, M.F.; Lopes, A.G.; De Nucci, G. Phase I Study of the Novel Antifungal Agent Dapaconazole (Zilt<sup>®</sup>) in Healthy Volunteers. *Int. J. Pharmacol.* **2014**, *10*, 507–512. [[CrossRef](#)]
3. Gobbato, A.A.M.; Gobbato, C.A.R.S.; Moreno, R.A.; Antunes, N.d.J.; De Nucci, G. Dapaconazole versus Ketoconazole in the Treatment of Interdigital Tinea Pedis. *Int. J. Clin. Pharmacol. Ther.* **2017**, *56*, 31–33. [[CrossRef](#)] [[PubMed](#)]
4. Gobbato, A.A.M.; Babadópulos, T.; Gobbato, C.A.R.S.; Ilha, J.O.; Antunes, N.J.; Moreno, R.A.; Campos, R.; De Nucci, G. Comparison of Dapaconazole with Miconazole in the Treatment of Tinea Cruris. *J. Eur. Acad. Dermatol. Venereol.* **2019**, *33*, 54–56. [[CrossRef](#)] [[PubMed](#)]
5. Gobbato, A.A.M.; Babadópulos, T.; Gobbato, C.A.R.S.; Ilha, J.D.O.; Gagliano-Jucá, T.; De Nucci, G. A Randomized Double-Blind, Non-Inferiority Phase II Trial, Comparing Dapaconazole Tosylate 2% Cream with Ketoconazole 2% Cream in the Treatment of Pityriasis Versicolor. *Expert Opin. Investig. Drugs* **2015**, *24*, 1399–1407. [[CrossRef](#)] [[PubMed](#)]
6. Keppler, A.F.; Sacurai, S.L.; Zaim, M.H.; Touzarim, C.E.C. Benzyl Aralkyl Ether Compounds, Method for Preparing Same, Intermediate Compounds, Use of Said Compounds, Method for Treatment and/or Prevention, Pharmaceutical Composition and Medicament Containing Same. U.S. Patent No. 8,975,289, 10 March 2015.
7. Palo, J.S.; De Freitas, N.L.; Silva, S.G.N.; Rojas-moscoso, J.A.; Za, T.; Lescano, C.H.; Mendes, G.D.; De Nucci, G. Pharmacokinetics of Dapaconazole, A Novel Antifungal Agent, in Beagle Dogs and Inhibition of Cytochrome P450 Family 51. *Anti-Infect. Agents* **2018**, *51*, 15–21. [[CrossRef](#)]

8. Gustafson, C.; Koslosky, M.; Leslie, J.; Walczak, C. Antifungal and Oral Anticancer Therapy Drug Interactions. *Curr. Fungal Infect. Rep.* **2020**, *14*, 130–140. [[CrossRef](#)]
9. Niwa, T.; Imagawa, Y.; Yamazaki, H. Drug Interactions between Nine Antifungal Agents and Drugs Metabolized by Human Cytochromes P450. *Curr. Drug Metab.* **2014**, *15*, 651–679. [[CrossRef](#)]
10. Yu, J.; Zhou, Z.; Owens, K.H.; Ritchie, T.K.; Ragueneau-Majlessi, I. What Can Be Learned from Recent New Drug Applications? A Systematic Review of Drug Interaction Data for Drugs Approved by the US FDA in 2015. *Drug Metab. Dispos.* **2017**, *45*, 86–108. [[CrossRef](#)]
11. Caldwell, G.W.; Yan, Z. *Optimization in Drug Discovery*, 2nd ed.; Caldwell, G.W., Yan, Z., Eds.; Methods in Pharmacology and Toxicology; Humana Press: Totowa, NJ, USA, 2014; ISBN 9781627037419.
12. Sudsakorn, S.; Bahadduri, P.; Fretland, J.; Lu, C. 2020 FDA Drug-Drug Interaction Guidance: A Comparison Analysis and Action Plan by Pharmaceutical Industrial Scientists. *Curr. Drug Metab.* **2020**, *21*, 403–426. [[CrossRef](#)]
13. FDA, U.S. Guidance for Industry: In Vitro Drug Interaction Studies—Cytochrome P450 Enzyme and Transporter Mediated Drug Interactions. Available online: <https://www.fda.gov/media/134582/download> (accessed on 24 November 2021).
14. Antunes, N.J.; Coombes, G.; Cunha, K.F.; Moreira, F.L.; Pilon, A.; Lopes, N.P.; Costa, J.L.; Kipper, K.; Couchman, L.; Johnston, A.; et al. In Vitro Metabolism of the New Antifungal Dapaconazole using liver microsomes. *Drug Metab. Pharmacokinet.* **2022**, *47*, 100475. [[CrossRef](#)] [[PubMed](#)]
15. Rodgers, T.; Rowland, M. Physiologically Based Pharmacokinetic Modelling 2: Predicting the Tissue Distribution of Acids, Very Weak Bases, Neutrals and Zwitterions. *J. Pharm. Sci.* **2006**, *95*, 1238–1257. [[CrossRef](#)] [[PubMed](#)]
16. Zou, P.; Zheng, N.; Yang, Y.; Yu, L.X.; Sun, D. Prediction of Volume of Distribution at Steady State in Humans: Comparison of Different Approaches. *Expert Opin. Drug Metab. Toxicol.* **2012**, *8*, 855–872. [[CrossRef](#)]
17. Cho, H.Y.; Choi, G.W.; Lee, Y.B. Interpretation of Non-Clinical Data for Prediction of Human Pharmacokinetic Parameters: In Vitro-in Vivo Extrapolation and Allometric Scaling. *Pharmaceutics* **2019**, *11*, 168. [[CrossRef](#)]
18. Peters, S.A.; Schroeder, P.E.; Giri, N.; Dolgos, H. Evaluation of the Use of Static and Dynamic Models to Predict Drug-Drug Interaction and Its Associated Variability: Impact on Drug Discovery and Early Development. *Drug Metab. Dispos.* **2012**, *40*, 1495–1507. [[CrossRef](#)] [[PubMed](#)]
19. Hua, L.; Chiang, C.W.; Cong, W.; Li, J.; Wang, X.; Cheng, L.; Feng, W.; Quinney, S.K.; Wang, L.; Li, L. The Cancer Drug Fraction of Metabolism Database. *CPT Pharmacomet. Syst. Pharmacol.* **2019**, *8*, 511–519. [[CrossRef](#)] [[PubMed](#)]
20. Siu, Y.A.; Lai, W.G. Impact of Probe Substrate Selection on Cytochrome P450 Reaction Phenotyping Using the Relative Activity Factor. *Drug Metab. Dispos.* **2017**, *45*, 183–189. [[CrossRef](#)]
21. Lempers, V.J.C.; Martial, L.C.; Schreuder, M.F.; Blijlevens, N.M.; Burger, D.M.; Aarnoutse, R.E.; Brüggemann, R.J.M. Drug-Interactions of Azole Antifungals with Selected Immunosuppressants in Transplant Patients: Strategies for Optimal Management in Clinical Practice. *Curr. Opin. Pharmacol.* **2015**, *24*, 38–44. [[CrossRef](#)]
22. Subramanian, M.; Tracy, T.S. Methods for Determination of Enzyme Kinetics and Metabolic Rates. In *Encyclopedia of Drug Metabolism and Interactions*; John Wiley & Sons, Inc.: Hoboken, NJ, USA, 2012; Volume 17, pp. 99–102.
23. Wang, H.; Huang, H.; Li, H.; Teotico, D.G.; Sinz, M.; Baker, S.D.; Staudinger, J.; Kalpana, G.; Redinbo, M.R.; Mani, S. Cancer Therapy: Preclinical Activated Pregnenolone X-Receptor Is a Target for Ketoconazole and Its Analogs. *Clin. Cancer Res.* **2007**, *13*, 2488–2496. [[CrossRef](#)]
24. Sakaeda, T.; Iwaki, K.; Kakumoto, M.; Nishikawa, M.; Niwa, T.; Jin, J.; Nakamura, T.; Nishiguchi, K.; Okamura, N.; Okumura, K. Effect of Micafungin on Cytochrome P450 3A4 and Multidrug Resistance Protein 1 Activities, and Its Comparison with Azole Antifungal Drugs. *J. Pharm. Pharmacol.* **2005**, *57*, 759–764. [[CrossRef](#)]
25. Monostory, K.; Hazai, E.; Vereczkey, L. Inhibition of Cytochrome P450 Enzymes Participating in p-Nitrophenol Hydroxylation by Drugs Known as CYP2E1 Inhibitors. *Chem. Interact.* **2004**, *147*, 331–340. [[CrossRef](#)] [[PubMed](#)]
26. Lamb, D.C.; Kelly, D.E.; Baldwin, B.C.; Kelly, S.L. Differential Inhibition of Human CYP3A4 and *Candida Albicans* CYP51 with Azole Antifungal Agents. *Chem. Interact.* **2000**, *125*, 165–175. [[CrossRef](#)] [[PubMed](#)]
27. Youdim, K.A.; Lyons, R.; Payne, L.; Jones, B.C.; Saunders, K. Journal of Pharmaceutical and Biomedical Analysis An Automated, High-Throughput, 384 Well Cytochrome P450 Cocktail IC 50 Assay Using a Rapid Resolution LC—MS/MS End-Point. *J. Pharm. Biomed. Anal.* **2008**, *48*, 92–99. [[CrossRef](#)] [[PubMed](#)]
28. Baldwin, S.J.; Clarke, S.E.; Chenery, R.J. Characterization of the Cytochrome P450 Enzymes Involved in the in Vitro Metabolism of Rosiglitazone. *Br. J. Clin. Pharmacol.* **1999**, *48*, 424–432. [[CrossRef](#)] [[PubMed](#)]
29. Carrão, D.B.; Habenbusch, M.D.; de Albuquerque, N.C.P.; da Silva, R.M.; Lopes, N.P.; de Oliveira, A.R.M. In Vitro Inhibition of Human CYP2D6 by the Chiral Pesticide Fipronil and Its Metabolite Fipronil Sulfone: Prediction of Pesticide-Drug Interactions. *Toxicol. Lett.* **2019**, *313*, 196–204. [[CrossRef](#)]
30. Habenschus, M.D. Estudos de Inibição Das Enzimas Do Citocromo P450 Pelo Produto Natural (–)-Grandisina Utilizando Microsomas Hepáticos de Humanos. Thesis, University of Sao Paulo, Ribeirao Preto, Brazil, 2016. Volume 127. Available online: [https://www.teses.usp.br/teses/disponiveis/59/59138/tde-06072016-095943/publico/Dissertacao\\_Maisa\\_versao\\_resumida\\_corrigida.pdf](https://www.teses.usp.br/teses/disponiveis/59/59138/tde-06072016-095943/publico/Dissertacao_Maisa_versao_resumida_corrigida.pdf) (accessed on 17 September 2021).
31. Walsky, R.L.; Obach, R.S. Validated Assays for Human Cytochrome P450 Activities. *Drug Metab. Dispos.* **2004**, *32*, 647–660. [[CrossRef](#)]

32. Walsky, R.L.; Obach, R.S.; Gaman, E.A.; Gleeson, J.P.R.; Proctor, W.R. Selective Inhibition of Human Cytochrome P4502C8 by Montelukast. *Drug Metab. Dispos.* **2005**, *33*, 413–418. [[CrossRef](#)]
33. Walsky, R.L.; Gaman, E.A.; Obach, R.S. Examination of 209 Drugs for Inhibition of Cytochrome P450 2C8. *J. Clin. Pharmacol.* **2005**, *45*, 68–78. [[CrossRef](#)]
34. Walsky, R.L.; Obach, R.S. A Comparison of 2-Phenyl-2-(1-Piperidinyl)Propane (PPP), 1,1',1''-Phosphinothioylidynetrisaziridine (ThioTEPA), Clopidogrel, and Ticlopidine as Selective Inactivators of Human Cytochrome P450 2B6. *Drug Metab. Dispos.* **2007**, *35*, 2053–2059. [[CrossRef](#)]
35. Dierks, E.A.; Stams, K.R.; Lim, H.K.; Cornelius, G.; Zhang, H.; Ball, S.E. A Method for the Simultaneous Evaluation of the Activities of Seven Major Human Drug-Metabolizing Cytochrome P450s Using an in Vitro Cocktail of Probe Substrates and Fast Gradient Liquid Chromatography Tandem Mass Spectrometry. *Drug Metab. Dispos.* **2001**, *29*, 23–29.
36. Rowland Yeo, K.; Jamei, M.; Yang, J.; Tucker, G.T.; Rostami-Hodjegan, A. Physiologically Based Mechanistic Modelling to Predict Complex Drug-Drug Interactions Involving Simultaneous Competitive and Time-Dependent Enzyme Inhibition by Parent Compound and Its Metabolite in Both Liver and Gut-The Effect of Diltiazem on the Time-C. *Eur. J. Pharm. Sci.* **2010**, *39*, 298–309. [[CrossRef](#)] [[PubMed](#)]
37. Rodrigues, A.D. *Drug-Drug Interactions (Drugs and the Pharmaceutical Sciences)*, 2nd ed.; Rodrigues, A.D., Ed.; CRC Press Informa Healthcare: London, UK, 2007; Volume 179, ISBN 10: 0-8493-7593-2.
38. FDA, U.S. Guidance for Industry: Clinical Drug Interaction Studies—Cytochrome P450 Enzyme- and Transporter-Mediated Drug Interactions. Available online: <https://www.fda.gov/Drugs/GuidanceComplianceRegulatoryInformation/Guidances/default.htm%0Ahttps://www.fda.gov/media/134581/download> (accessed on 24 November 2021).

**Disclaimer/Publisher's Note:** The statements, opinions and data contained in all publications are solely those of the individual author(s) and contributor(s) and not of MDPI and/or the editor(s). MDPI and/or the editor(s) disclaim responsibility for any injury to people or property resulting from any ideas, methods, instructions or products referred to in the content.